

## Multicellular systems biology

Bassel, George W.

DOI:

[10.1016/j.molp.2019.02.004](https://doi.org/10.1016/j.molp.2019.02.004)

License:

Creative Commons: Attribution-NonCommercial-NoDerivs (CC BY-NC-ND)

*Document Version*

Peer reviewed version

*Citation for published version (Harvard):*

Bassel, GW 2019, 'Multicellular systems biology: quantifying cellular patterning and function in plant organs using network science', *Molecular Plant*, vol. 12, no. 6, pp. 731-742. <https://doi.org/10.1016/j.molp.2019.02.004>

[Link to publication on Research at Birmingham portal](#)

### General rights

Unless a licence is specified above, all rights (including copyright and moral rights) in this document are retained by the authors and/or the copyright holders. The express permission of the copyright holder must be obtained for any use of this material other than for purposes permitted by law.

- Users may freely distribute the URL that is used to identify this publication.
- Users may download and/or print one copy of the publication from the University of Birmingham research portal for the purpose of private study or non-commercial research.
- User may use extracts from the document in line with the concept of 'fair dealing' under the Copyright, Designs and Patents Act 1988 (?)
- Users may not further distribute the material nor use it for the purposes of commercial gain.

Where a licence is displayed above, please note the terms and conditions of the licence govern your use of this document.

When citing, please reference the published version.

### Take down policy

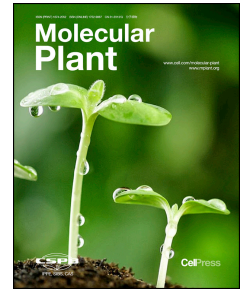
While the University of Birmingham exercises care and attention in making items available there are rare occasions when an item has been uploaded in error or has been deemed to be commercially or otherwise sensitive.

If you believe that this is the case for this document, please contact [UBIRA@lists.bham.ac.uk](mailto:UBIRA@lists.bham.ac.uk) providing details and we will remove access to the work immediately and investigate.

# Accepted Manuscript

Multicellular systems biology: quantifying cellular patterning and function in plant organs using network science

George W. Bassel



PII: S1674-2052(19)30058-9  
DOI: <https://doi.org/10.1016/j.molp.2019.02.004>  
Reference: MOLP 744

To appear in: *MOLECULAR PLANT*  
Accepted Date: 14 February 2019

Please cite this article as: **Bassel G.W.** (2019). Multicellular systems biology: quantifying cellular patterning and function in plant organs using network science. *Mol. Plant*. doi: <https://doi.org/10.1016/j.molp.2019.02.004>.

This is a PDF file of an unedited manuscript that has been accepted for publication. As a service to our customers we are providing this early version of the manuscript. The manuscript will undergo copyediting, typesetting, and review of the resulting proof before it is published in its final form. Please note that during the production process errors may be discovered which could affect the content, and all legal disclaimers that apply to the journal pertain.

All studies published in *MOLECULAR PLANT* are embargoed until 3PM ET of the day they are published as corrected proofs on-line. Studies cannot be publicized as accepted manuscripts or uncorrected proofs.

1 **TITLE**

2 Multicellular systems biology: quantifying cellular patterning and function in plant organs using  
3 network science

4

5

6 **AUTHORS/AFFILIATIONS**

7 George W. Bassel<sup>1,\*</sup>

8 <sup>1</sup>School of Biosciences, University of Birmingham, Birmingham B15 2TT, UK;

9 **CORRESPONDING/LEAD AUTHOR**

10 \*To whom correspondence should be addressed: [g.w.bassel@bham.ac.uk](mailto:g.w.bassel@bham.ac.uk) (G.W.B) School of  
11 Biosciences, University of Birmingham, Birmingham B15 2TT, UK, +44 (0)121 41 42502;

12

13 **ABSTRACT**

14 Organ function is at least partially shaped and constrained by the organization of their  
15 constituent cells. Extensive investigation has revealed mechanisms explaining how these  
16 patterns are generated, with less being known about their functional relevance. In this paper, a  
17 methodology to discretize and quantitatively analyze cellular patterning is described. By  
18 performing global organ-scale cellular interaction mapping, the organization of cells can be  
19 extracted and analyzed using network science. This provides a means to take the  
20 developmental analysis of cellular organization in complex organisms beyond qualitative  
21 descriptions, and provides data-driven approaches to inferring cellular function. The bridging of  
22 a structure-function relationship in hypocotyl epidermal cell patterning through global topological  
23 analysis provides support for this approach. The analysis of cellular topologies from patterning  
24 mutants further enables the contribution of gene activity towards the organizational properties of  
25 tissues to be linked, bridging molecular and tissue scales. This systems-based approach to  
26 investigate multicellular complexity paves the way to uncovering the principles of complex organ  
27 design, and achieving predictive genotype-phenotype mapping.

28

29

30 **KEYWORDS**

31 Organ, network, connectivity, transport, tissue topology, connectome

## 32 Introduction

33 Organs are self-contained collections of interacting cells that perform a function that individual  
34 cells cannot (Bonner, 1988). Through the process of emergence, these multicellular consortia  
35 give rise to complex life (Solé and Goodwin, 2000). What organs are capable of achieving is at  
36 least partially shaped and constrained by structure-function relationships at the cellular level  
37 such that their organization impacts their collective performance (Ollé-Vila et al., 2016;  
38 Thompson, 1942).

39 Previous studies have identified principles and mechanisms by which patterns are created in  
40 plants, including the contribution of each genetic pathways and biophysical forces (Gaillochet et  
41 al., 2015; Hamant et al., 2008). The use of genetic mutant screens have identified molecular  
42 agents that underpin the active control of specific cell divisions that give rise to cell  
43 arrangements, and provide key insight into how local arrangements of cells are created  
44 (DiLaurenzio et al., 1996; Hardtke and Berleth, 1998).

45 The immobility of cells in plant tissues makes the combination of the control of the cell cycle,  
46 and orientation of the division plane, the key factors defining cellular organization (Meyerowitz,  
47 1997). Given these constraints, asymmetric divisions are sufficient to generate novel  
48 arrangements (De Smet and Beeckman, 2011; Dong et al., 2009; Smith, 2001). Several  
49 examples of this include the formation of stomata (Raissig et al., 2017), the creation hypophysis  
50 during embryo development (Schlereth et al., 2010), and cell divisions leading to cortical and  
51 endodermal cell layers during root development (DiLaurenzio et al., 1996).

52 These studies provide detailed and mechanistic insights as to how local arrangements of cells  
53 are generated. How these groups of cells come together to form a global integrated system of  
54 interacting cells at the organ scale, is less well understood. The functional consequences  
55 cellular organization has on organ function and structure-function relationships at this scale also  
56 represents a knowledge gap. In order to address these questions, a discrete and quantitative  
57 approach to extract and analyze cellular architecture is required.

58 Anatomical analyses have historically provided largely qualitative descriptions of tissues, with  
59 quantitative approaches to analyzing structure rapidly being developed. Methods to analyze cell  
60 shape (Pincus and Theriot, 2007; Sánchez-Corrales et al., 2018), curvature across organs  
61 (Kierzkowski et al., 2012), and root systems (Fang et al., 2013) in quantitative ways have been  
62 applied previously. Gaps remain in understanding organ level organizational properties at a  
63 cellular level.

64 An approach that has been transformative to understanding nervous system structure and  
65 function is that of cellular interaction mapping (Ramon y Cajal, 1911) and “connectomics”

66 (Sporns et al., 2005). By performing cellular interaction mapping of neurons, the organizational  
67 properties of nervous systems, and function of individual neurons, has been predicted (Chalfie  
68 et al., 1985).

69 In this article an extension of connectionist approaches to analyzing cellular organization is  
70 proposed. This creates for a “systems biology of the organ”, opening the door to a host of  
71 investigative opportunities provided by network and complexity science.

72

### 73 **The origins of cellular interaction mapping**

74 The advent of cellular interaction mapping can be traced to Ramon y Cajal (Ramon y Cajal,  
75 1911). By staining tissues with a Golgi stain and performing light microscopy, Cajal was able to  
76 visualize the connections between individual neurons in various animal tissues. A more  
77 systematic approach was later taken to comprehensively map each of the 302 neurons and their  
78 connections within the worm *C. elegans* (White et al., 1986). This resulted in the production of  
79 the first “wiring diagram”, a network describing global neuronal connectivity (connectome)  
80 (Sporns et al., 2005). In the case of such an interaction network, cells are represented by  
81 nodes, and their physical associations as edges. The network-based analyses of this dataset  
82 has proven sufficient to predict the function of individual neurons in touch sensitivity (Chalfie et  
83 al., 1985), and motor control (Yan et al., 2017). The only other completed neuronal connectome  
84 to date has come from the sea squirt, 30 years after that of *C. elegans*, and contains 177  
85 neurons (Ryan et al., 2016).

86 The topological analysis of connectomes has been sufficient to predict the function of individual  
87 cells in nervous systems in *C. elegans*, demonstrating the ability to bridge structure-function  
88 relationships in cellular consortia using network science. While a neuron is one of many cell  
89 types which contribute to the construction of complex animals, many organisms including plants,  
90 don't have nervous systems, and consist of collections of diverse cells types upon which  
91 information may be processed (Baluška and Levin, 2016; Bassel, 2018). The investigation of  
92 relationships between cell organization and function in non-neuronal systems remains largely  
93 unexplored.

94

### 95 **Organs as integrated systems of interacting cells**

96 Communication between cells underpins the emergent behaviour of organs (Solé and Goodwin,  
97 2000). Multicellular plants may therefore be viewed as integrated multicellular transport  
98 systems. In these systems, mobile information may be any developmentally instructive  
99 molecule, which can include mRNA (Lucas et al., 1995), miRNA (Carlsbecker et al., 2010),

100 proteins (Nakajima et al., 2001), ions (Knight et al., 1991), hormones (Swarup et al., 2001; Tal  
101 et al., 2016), and peptides (Ogawa et al., 2008). Networks describing the connectivity between  
102 cells capture the possible routes of information movement across the organ.

103 Symplastic connections between cells, mediated by plasmodesmata, represent a primary  
104 means of information movement between cells (Brunkard and Zambryski, 2017; Fitzgibbon et  
105 al., 2013; Lucas and Lee, 2004). Cells also communicate through specific membrane-bound  
106 transporters, and their intercellular space termed the apoplast (Blilou et al., 2005). In these latter  
107 cases, the proximity between adjacent cells plays a key role in determining the destination of  
108 extracellular mobile information, making cellular proximity and association relevant in these  
109 instances as well.

110

### 111 **Abstraction of plant organs into cellular interaction networks**

112 In order to identify physical associations between cells in plant organs, image-based  
113 approaches may be applied (Figure 1). Imaging techniques involving clarification of fixed tissue  
114 provide a means to perform whole organ cellular resolution imaging that is otherwise limited by  
115 optical aberration of laser light (Kurihara et al., 2015; Palmer et al., 2015; Truernit et al., 2008).  
116 These techniques enable all cells in entire organs to be digitally captured in 3D from z-stacks  
117 using confocal microscopy. In contrast to neuronal connectomics which focuses on a single cell  
118 type, this approach focuses on all cells within the organ, providing a comprehensive approach to  
119 understanding global structure of these multicellular systems.

120 The abstraction of these image volumes into networks describing cellular interactions requires  
121 computational image analysis (Bassel and Smith, 2016; Roeder et al., 2012; Roeder et al.,  
122 2011). Cells are segmented in 3D, and surfaces are defined using polygonal meshes (Cuno et  
123 al., 2004), leading to the identification of nodes in the network. Cell surfaces which are in  
124 physical association with one another are identified, enabling the establishment of edges  
125 (Montenegro-Johnson et al., 2015). The geometric size of these shared intercellular interfaces  
126 can be quantified based on the amount of shared interface between cell pairs. The output of this  
127 analysis comes in the form of a text file describing the pairwise interactions between cells in the  
128 organ analyzed.

129 The physical nature of this image analysis provides robust datasets, which are both accurate  
130 and reproducible (Jackson et al., 2017b; Yoshida et al., 2014). In contrast to other biological  
131 interaction network data which are often incomplete and subject to inaccuracies due to false  
132 positives and negatives (Von Mering et al., 2002), cellular interactome datasets capture all cells  
133 and interactions with high confidence due to the physical nature of the measurements. The

134 complete nature of these datasets (capturing the entire system) further provides powerful  
135 opportunities to perform quantitative network-based analyses to explore the system-wide  
136 properties with high confidence given no aspects of the system are missing. The further  
137 identification of cell types within cellular representations of organs, using for example  
138 3DCellAtlas (Montenegro-Johnson et al., 2015), enables cell type specific topological analyses  
139 to be performed (Jackson et al., 2017b).

140

#### 141 **Topological analysis of plant cellular interaction networks**

142 Unlike animal tissues where cells move around, cells in plant organs are fixed in their position  
143 (Coen et al., 2004). This renders cellular organization topologically invariant, and simplifies the  
144 analysis of these static cellular arrangements. Cells are typically tessellated within plant organs,  
145 with some notable exceptions such as the leaf, where air spaces are formed. The lattice-like  
146 nature of these cellular arrangements provides templates upon which molecular events take  
147 place.

148 The topological analysis of networks describing plant cellular organization can be performed at  
149 each local and global scales (Jackson et al., 2017a; Jackson et al., 2017b). The simplest local  
150 question that can be asked is how many direct neighbours a cell has. In network terminology,  
151 this is termed degree (Barabási, 2016; Newman, 2010), and measures how much local  
152 influence an individual cell has at a given location within an organ (Figure 2B). The degree of  
153 cells has been explored in the context of animal and plant epithelia previously, and described in  
154 terms of polygons (Carter et al., 2017; Gibson et al., 2006; Gibson et al., 2011; Sahlin and  
155 Jönsson, 2010). The polygonal count of these cells is a readout of their number of neighbours,  
156 and was demonstrated to converge on a distribution centering at the number six. The cell  
157 cleavage plane in the *Drosophila* imaginal wing disc and cucumber shoot apical meristem  
158 (SAM) was further shown to have a bias towards intersecting the neighbouring cell having the  
159 lowest degree, thus increasing the number of neighbours of this adjacent cell (Gibson et al.,  
160 2011). It was proposed that this generative process leads to the maintenance of topological  
161 order in these tissues.

162 While informative, degree does not capture the role of cells within the broader context of  
163 multicellular systems (Barabási, 2016). In light of the immobility and spatial constraints on these  
164 multicellular transport networks, the property of path length represents a biologically significant  
165 topological feature (Barthélemy, 2011). On a local scale, cells are only able to directly  
166 communicate with their immediate neighbours. On the global scale, cells are indirectly in contact



167 with one another through other intermediary cells, a property which may play a functional role in  
168 organ function.

169 In traversing a network, optimal routing is to follow a shortest path between two nodes,  
170 representing the minimum number of edges travelled (Barabási, 2016; Newman, 2010). The  
171 same applies to plant organs where molecular movement within a cytoplasm is less costly than  
172 passing through cell interfaces. Cells which lie upon shortest paths between other pairs of cells  
173 are therefore able to control the flow of information across an organ.

174 Network centrality measures have been developed which are capable of identifying nodes that  
175 lie upon a greater number of shortest paths between other pairs of nodes. Betweenness  
176 centrality (BC) uses prior knowledge of the complete network to calculate the shortest paths  
177 between all pairs of nodes (Freeman, 1977) (Figure 2C). Cells which lie upon a greater number  
178 of shortest paths between other cell pairs have a higher BC.

179 Random Walk Centrality (RWC) does not use prior knowledge of the system to calculate  
180 shortest paths. Source nodes send out many random walkers and track which nodes are  
181 traversed until they reach their destination (Newman, 2005) (Figure 2D). Nodes which are  
182 traversed more frequently are given a greater RWC. Very large number of random walkers are  
183 required to identify high RWC paths as a minority of individual agents follow near-optimal routes  
184 due to their random motion.

185 In the case of both BC and RWC, having a greater value increases the ability of a cell to control  
186 information flow across an organ as it identifies cells lying upon a greater number of shortest  
187 paths. This represents a biologically relevant property of organs in light of the system-wide  
188 communication which takes place.

189 The application of global topological analyses including BC and RWC to plant connectomes is  
190 appropriate when these systems are fully represented, with all cells and interactions present.  
191 The ability to derive meaningful results from partial or inaccurate datasets using global  
192 calculations is limited given the global reach of these measures.

193 The identification of a shortest path in a network without prior knowledge of its topology  
194 represents a complex logistical problem. This is equivalent to identifying optimal routes in  
195 navigating a city without a map. This scenario is encountered by tissues, as they do not have  
196 information as to where all other cells are located within an organ. A recently developed  
197 measure named Navigation Centrality (NC) (Seguin et al., 2018), analogous to Greedy  
198 Navigation (Muscoloni and Cannistraci, 2019; Muscoloni et al., 2017) provides a simple  
199 propagation rule that is able to identify near optimal shortest paths using only local information.  
200 By integrating the geometric information as to how nodes are embedded in space, progressive

201 steps following a gradient to a destination is followed (Figure 2E). NC therefore provides a  
202 biologically realistic calculation to identify optimal routes which are not provided by other  
203 measures such as BC and RWC. This centrality has yet to be applied to multicellular tissues  
204 outside of the nervous system, yet provides a promising approach in light of the nature by which  
205 the calculation is performed.

206 Another biologically relevant consideration in the analysis of multicellular tissues is the efficiency  
207 by which they can exchange information (Barabási, 2016). This may be considered at each the  
208 local and global scales (Latora and Marchiori, 2001). The global measure considers how  
209 efficient a whole system is at transmitting information, while local efficiency quantifies the  
210 resilience of this information movement on a small scale in the face of individual failures. A  
211 tradeoff between global and local efficiency and the optimization between each of these in  
212 different contexts represents an important design feature in diverse transport systems, and  
213 provides another promising approach to understanding tissue architecture.

214 Several caveats in the analysis of cellular interaction network datasets must be considered.  
215 Input datasets need to be carefully curated to ensure their maximal accuracy and completeness.  
216 The lattice-like nature of these networks and the small number of nodes and edges lead small  
217 inaccuracies to have large consequences on subsequent analyses. In order to achieve robust  
218 global path length-based analyses, fully accurate networks are required (Barthélemy, 2011).

219 A second caveat lies with the nature of topological analyses performed. It necessary to consider  
220 the calculation that is made and its relevance to biology. How a cell calculates its number of  
221 neighbours remains an outstanding question (Gibson and Gibson, 2009), while centralities such  
222 as BC are not biologically feasible as plants lack maps of their cellular organization (Baluška  
223 and Levin, 2016). Despite the biological challenges associated with both degree and BC, their  
224 measurement still provides important insight into the organization of cells in organ, while the  
225 manner in which they are interpreted requires the appropriate caution.

226

### 227 **Structural and functional networks**

228 The capture and abstraction of global cellular interactions into networks is analogous to the  
229 creation of a map describing a transport system such as a rail network (Barthélemy, 2011). All  
230 the routes of possible movement are described by the representation.

231 In the context of cellular interactomes, these are termed *structural networks*, and describe the  
232 possible routes of information flow across an organ (Figure 3A) (Bullmore and Sporns, 2009).  
233 Following this rail system analogy, these maps do not provide a schedule indicating the

234 timetable or speed of the trains. In order to achieve this, functional annotation of the map with  
235 additional information is required.

236 A *functional network* is a structural network that has been annotated with additional dimensions  
237 of data (Bullmore and Sporns, 2009) (Figures 3B-C). In the case of a plant connectome,  
238 functional annotation could include information relating to either the nodes (cells) (Figure 3B) or  
239 the edges (interfaces) (Figure 3C), or both, depending on what is being investigated.

240 Node annotation may include different data types, including for example the abundance of a  
241 protein within a cell, or the intensity of a biosensor. The application of these data to the network  
242 involves the additional of a value to an individual node (Figure 3B).

243 Edge annotation may include the presence and/or abundance of a transporter, the abundance  
244 of plasmodesmata/pit fields on cell interfaces, or the size of cell interfaces. Functional  
245 annotation of plasmodesmata aperture can also be evaluated by measuring the rates of  
246 movement of fluorescent molecules between adjacent cells (Gerlitz et al., 2018). The application  
247 of these data to a network data structure involves the addition of values to edges (Figure 3C).

248 Understanding each the abundance and aperture of plasmodesmata on intercellular interfaces  
249 is central to understanding system-wide organ communication. While structural templates  
250 provide routes of possible information flow, functional annotation represents that which is  
251 observed to occur. With this in mind, two cells which are physically associated are not  
252 necessarily communicating. In order for that to occur there both needs to be plasmodesmata  
253 present, and they also need to be open. Symplastic connections are dynamic and change  
254 across plant development (Rinne et al., 2001; Rinne et al., 2011), indicating that functional  
255 annotation itself is temporal in nature (Holme and Saramäki, 2012).

256 The functional annotation of plant connectomes may be greatly aided by techniques involving  
257 the gel-based embedding of tissues including PEA-CLARITY (Palmer et al., 2015). This  
258 technique enables the repeated localization of molecular components within tissues through  
259 repeated rounds whole mount *in situ* hybridization using antibodies and/or oligonucleotides.  
260 Samples may repeatedly be stripped and reprobbed, analogous to a western blot membrane.  
261 This provides a highly multidimensional functional annotation with multiple rounds of probing of  
262 the same sample, and transcends the limits imposed by resolving individual fluorophores using  
263 confocal microscopy.

264 With the functional annotation of networks comes additional values which can be integrated into  
265 centrality measurements. These centralities are in turn calculated using these “weighted”  
266 values, and simultaneously integrate both the organization of cells and their functional  
267 properties in the outputs.

268

269 **Case study 1: the plant hypocotyl**

270 Global structural cellular interaction mapping has been applied to understanding the  
271 organization of cells in the plant hypocotyl (Jackson et al., 2017b). Following the germination of  
272 the embryo, cells in the hypocotyl elongate to promote seedling development, in the absence of  
273 cell divisions (Gendreau et al., 1997; Sliwinska et al., 2009). Similar to the root, cells in the  
274 hypocotyl have a radial and modular organization (Figure 4A). In both organs, two cell types are  
275 present in the epidermis: trichoblasts which produce hairs which promote nutrient uptake, and  
276 atrichoblasts which are adjacent to trichoblasts but do not produce hairs. Studies have  
277 uncovered detailed genetic mechanisms that lead to the formation of these two cell types,  
278 describing how epidermal patterning is generated (Dolan, 2005; Duckett et al., 1994). The  
279 functional relevance of the stereotyped pattern of these two cell types is less well understood.

280 An attempt to bridge structure and function in epidermal cell organization was undertaken using  
281 a connectionist approach (Jackson et al., 2017b). Whole mount 3D imaging of fixed samples  
282 resulted in the capture and discretization of cellular connectivity in this organ. Individual cell  
283 types were identified (Figure 4A) (Montenegro-Johnson et al., 2015) in quadruplicate biological  
284 replicates enabling cell type specific topological analyses of patterning to be performed together  
285 with statistical analyses.

286 In the *Arabidopsis* hypocotyl epidermis it was found that trichoblasts had more neighbours  
287 (higher degree) than atrichoblasts (Figure 4B). Contributing to this is their position above two  
288 underlying cortical cells, in contrast to atrichoblasts which are above one (Figure 4A). Path  
289 length calculation revealed that atrichoblasts have a higher BC than trichoblasts (Figure 4C).  
290 Despite having fewer neighbours, atrichoblasts lie upon a greater number of shortest paths than  
291 their counterparts. This represents a non-intuitive higher-order property of epidermal patterning  
292 in the hypocotyl, and the presence of conduits of reduced path length along the longitudinal axis  
293 of this organ.

294 The functional relevance of these conduits of reduced path length was examined by placing  
295 seedlings onto media containing fluorescein and imaging using confocal microscopy to identify  
296 where it moves (Duran-Nebreda and Bassel, 2017b). Bulk molecular movement of the  
297 fluorescein molecule followed the identified shortest paths through the hypocotyl via the  
298 atrichoblast cell type (Figure 4D). Given a map of global cellular organization, BC is therefore  
299 sufficient as a topological proxy to predict molecular movement at single cell resolution through  
300 this complex multicellular plant system. The means by which this shortest path calculation is

301 performed in the biological context remains enigmatic, with Navigation Centrality providing a  
302 promising approach to understand how this may be achieved (Seguin et al., 2018).

303 These observations provide a potential link between structure and function in epidermal cell  
304 patterning in the hypocotyl in *Arabidopsis*. Each hair cell promotes solute uptake, and is flanked  
305 by 2 non-hair cells. The higher-order organization of non-hair cells facilitates them for the  
306 optimized longitudinal movement of molecules. A division of labour is therefore implemented  
307 whereby hair cells perform nutrient uptake, while non-hair cells aid transport (Figure 4E). This  
308 enables intracellular solute concentration to be kept low in trichoblast cells facilitating their  
309 uptake function, while providing optimized conduits for molecular movement on the surface of  
310 the organ. In this example, the analysis of a structural network alone is sufficient to predict cell  
311 function in the hypocotyl epidermis.

312 Analyses of biological quadruplicates from 3 different *Arabidopsis* ecotypes identified  
313 statistically significant genotype-specific differences epidermal path length (Jackson et al.,  
314 2017b). This demonstrates the presence of conserved emergent patterning properties at each  
315 the local and global scales in the hypocotyl, and the ability to reliably perform quantitative  
316 analyses of cellular global organization in plants using connectionist approaches. It further  
317 highlights the presence of patterning plasticity within the epidermis of the *Arabidopsis* hypocotyl  
318 in different genetic backgrounds which have higher-order organizational consequences. This  
319 plasticity may provide a means for modulating adaptive fitness at the organ design level in light  
320 of these structure-function relationships.

321

### 322 **Case study 2: the developing plant embryo**

323 Early embryo development in *Arabidopsis* was also investigated using a connectionist approach  
324 previously (Yoshida et al., 2014). The topological analysis of the 16 cell embryo was performed  
325 with a view to understanding how pairs of cells are connected to one another. To address this,  
326 the frequency of shared neighbours, the number of shared 1<sup>st</sup> degree connections between  
327 pairs of nodes (Assenov et al., 2007), was determined. This represents a mesoscopic analysis  
328 of the connectedness of a system.

329 Wild type embryos (Figure 5A) were compared with transgenic individuals expressing the  
330 *IAA12/BODENLOS (BDL)* gene (Figure 5B), which is a repressor of the *AUXIN RESPONSE*  
331 *FACTOR5* named *MONOPTEROS (MP)* (Hamann et al., 2002). *MP* has been demonstrated to  
332 carry defects in embryo patterning (Hardtke and Berleth, 1998), and plays a role in mediating  
333 the contribution of the hormone auxin towards creating this structure. *BDL* was placed under the  
334 control of the *RPS5A* promoter (*RPS5A::bdl*), supporting high level expression in the embryo.

335 The number of shared neighbours in the transgenic *RPS5A::bdl* expressing line was greater than  
336 that of the wild type embryo, indicating an overall increase in the connectedness of this system  
337 (Figure 5C). This provided a quantitative link between auxin signaling mediated by *MP* and the  
338 organization of cells in the developing embryo. The analysis of biological triplicate samples  
339 supported the robustness these mesoscale patterning properties in this tissue.

340

### 341 **Case study 3: the plant shoot apical meristem**

342 A recent study topologically investigated the organization of cells within the SAM at both local  
343 and global scales (Figure 6A) (Jackson et al., 2019). Time lapse live imaging was performed to  
344 examine the relationship between cellular organization and the control of the cell cycle. Cellular  
345 connectivity networks of cells in the SAM were extracted from images, and the topological  
346 dynamics of this network was established using image registration and lineage tracking (de  
347 Reuille et al., 2015; Fernandez et al., 2010).

348 Cells were separated into 3 classes: those which do not divide, cells which will divide, and  
349 daughter cells following divisions (Figure 6B). The volume of cells was capable of discriminating  
350 between these size classes, consistent with previous reports describing a size control  
351 mechanism for cells in the SAM (Jones et al., 2017; Willis et al., 2016). While cell shape  
352 (anisotropy) did not discriminate whether or not a cell would divide, the number of neighbours  
353 (degree) did, along with the number of shortest paths a cell lies upon (BC and RWC) (Figure  
354 6B). These data demonstrated cells in the SAM to be undergoing both geometric and  
355 topological cycling.

356 These observations further suggested that topology can be used to identify when a cell will  
357 divide, as cells that lie upon an increasing number of shortest paths are more likely to undergo a  
358 division. Following this division, the number of shortest paths the daughter cells is limited  
359 (Figure 6B), opening the possibility that the placement of a cell division plane may be predicted  
360 based on the global topology of the tissue.

361 Computational analysis of cell division planes based on the minimization of the degree and  
362 RWC of daughter cells was performed, along with the local geometric rule from Errera that  
363 divides a cell in half using the shortest possible wall which passes through the middle (Besson  
364 and Dumais, 2011; Errera, 1888) (Figure 6C). The local geometric rule of Errera and the global  
365 topological RWC Minimizing rule were found to largely both predict the same division plane, and  
366 show similar deviations from observed division planes (Figure 6D). The results collectively  
367 suggested that the local shape of a cell within the SAM predisposes it for a shortest wall division  
368 plane that also satisfies the minimization of RWC in the daughter cell



369 Intercellular interactions play a key role in the control of cell shape in plant tissues with cells  
370 being connected through shared cell walls (Coen et al., 2004). The microtubule severing protein  
371 *KATANIN1* (*KTN1*) has been demonstrated to mediate mechanical interactions between cells  
372 and regulate morphogenesis of the SAM (Uyttewaal et al., 2012). Geometric analysis of cell  
373 shape in the *ktn1* SAM demonstrated these to be more anisotropic than their counterparts in the  
374 wild type (Figure 6G) which in turn led to cells lying upon more shorter paths, based on  
375 increased RWC (Figure 6H). Mechanical interactions between cells therefore generate the cell  
376 shapes required for a local shortest wall division that in turn leads to the minimization of RWC in  
377 their cells (Figure 6I).

378 This mechanical feedback onto cell geometry and emergent generation of a tissue with  
379 minimized RWC identifies how local rules can lead to global properties. It further provides an  
380 example of complexity for free, whereby an emergent global system feature arises from simple  
381 local interactions. This example of emergent global topological order in the *Arabidopsis* SAM  
382 may extend to other tissue contexts, where division rules may either increase or limit the path  
383 length the daughter cells lie upon following their division.

384 The function implication of the minimization of RWC (maximization of path lengths traversed)  
385 across the SAM represents an optimization for the robustness of the system (increased local  
386 efficiency) at the cost communication speed (global efficiency), as no individual cells lie in  
387 privileged positions to facilitate rapid communication across the tissue. This may in turn impact  
388 the behaviour of this multicellular system in the face of perturbation, or internal failure.  
389 Topological homogeneity in the SAM also correlated with robustness in phylotaxis, as  
390 perturbations were observed in the *ktn1* mutant.

391

### 392 **Bridging molecular and cellular scales**

393 A quantitative approach to the analysis of cellular organization provides the opportunity to  
394 identify the consequences of altered arrangements in patterning mutants at local and global  
395 scales. In instances where the gene responsible for changes in cellular patterning is known, this  
396 represents a quantitative bridging of the molecular and cellular scales of plant development  
397 (Duran-Nebreda and Bassel, 2017a).

398 Examples of this have been described above, where a link between auxin-mediated signaling  
399 and connectivity in the 16 cell *Arabidopsis* embryo was identified (Figure 5C) (Yoshida et al.,  
400 2014), and mechanical feedbacks mediated by *KATANIN1* control cell shape and the path  
401 length upon which cells lie in the SAM (Figures 6G-I) (Jackson et al., 2019). These examples

402 provide quantitative links between genetic agents and the cellular configurations they contribute  
403 towards generating.

404 Ecotype-specific differences in the *Arabidopsis* hypocotyl were also identified with respect to the  
405 path length upon which epidermal cells lie (Jackson et al., 2017b). The functional relevance of  
406 these differences was demonstrated through the use of fluorescein transport assays which  
407 identified the preferential movement of molecules along cells lying upon shortest paths in this  
408 tissue. This relationship was faithfully followed across ecotypes having divergent path length  
409 differences between epidermal cell types.

410 Further quantitative analysis of altered cellular configurations were performed using *Arabidopsis*  
411 hypocotyls and the patterning mutants *CYCLIN DEPENDENT KINASEA1;1* (*CDKA1;1*)  
412 (Dissmeyer et al., 2009) and *MP* (Schlereth et al., 2010). *CDKA1;1* was found to have equal BC  
413 between hair and non-hair cells, while the BC of both epidermal cells types *MP* is significantly  
414 greater than the equivalent wild-type.

415

#### 416 **Genotype-phenotype mapping and meso scale analyses**

417 The ability to map genotype to phenotype represents a grand challenge in biology. The  
418 measurement of each genotype through sequencing, and downstream macro outputs through  
419 phenotyping, enables links between the molecular and organismal scales (Atwell et al., 2010).  
420 Our ability to do this in a predictive fashion remains limited, and may be due to gaps in our  
421 understanding as to the mechanistic basis by which genetic changes lead to phenotypic  
422 consequences. One means to bridge this gap is through the study of the “meso” scales of  
423 development, representing the events which occur between genotype and phenotype. These  
424 include, but are not limited to, intracellular behaviour, cellular organization, inter-organ  
425 communication, and how each of these in turn interact with the environment.

426 A quantitative view of organ architecture, and the pursuit of investigation to understand the  
427 functional consequences of cellular configurations, may contribute towards the bridging of  
428 scales and predictive genotype-phenotype mapping. An example of this potential is provided by  
429 the identification of ecotype-specific differences in epidermal patterning across ecotypes of the  
430 *Arabidopsis* hypocotyl (Jackson et al., 2017b). These differences had consequences in terms of  
431 the bulk movement of small molecules, and suggests the higher order properties of cellular  
432 organization may represent an axis upon which natural selection acts to optimize plant fitness.  
433 Further work in this area is required to establish the extent to which this occurs in different  
434 organs and species.

435



**436 Single cell sequencing and organ topology**

437 The ability to sequence individual cells across whole organs is providing unparalleled insight  
438 into the heterogeneity of gene expression within individual cell types, and the developmental  
439 trajectories they take as they acquire their identity (Birnbaum, 2018). While powerful, these  
440 approaches require the dissociation of tissue to isolate single cells for sequencing. If one seeks  
441 to understand how cells come together to create a functional integrated organ system, this loss  
442 of positional information and their relationships presents a boundary to achieving a  
443 multidimensional understanding.

444 The ability to perform single cell sequencing on intact tissue where relationships between cells  
445 are preserved would reconcile this gap. This was recently achieved in moss through the use of  
446 microcapillary manipulation (Kubo et al., 2018). Further technological advances promise to  
447 bridge this gap, including the integration of landmark genes (Halpern et al., 2017).

448

**449 Towards the principles of organ design**

450 The ability to abstract and discretize patterning into networks enables quantitative comparisons  
451 between diverse genotypes and species to be performed (Avena-Koenigsberger et al., 2015).  
452 The topological analysis of these distinct datasets coupled with statistical analyses may lead to  
453 the identification of shared and divergent properties in organ design, paving the way for an  
454 understanding of the principles of cellular architecture. Elucidating how cells come together to  
455 form organs, and how those arrangements shape and constrain tissue function is central to  
456 understanding multicellular complexity. Identifying properties that emerge “for free” by virtue of  
457 cells being embedded in space, versus the mechanisms that underpin deviations from these  
458 default configurations, represent key objectives in understanding multicellular development and  
459 realizing rational morphogenetic engineering (Doursat et al., 2012; Solé et al., 2018).

460

**461 Concluding remarks**

462 The application of connectionist approaches holds promise for plant developmental biology. The  
463 construction of whole organ structural networks has begun, and paves the way for their  
464 functional annotation by the collective efforts of the community. In this way, the manner by  
465 which cells and molecules interact to create an integrated system will increase our  
466 understanding of plant development. The bridging of scales from molecules to organs may  
467 facilitate quantitative genotype-phenotype mapping. The translational promise of this approach  
468 lies with its application to crop species, to which technical boundaries do not limit this extension.

469 By understanding the context in which genetic programs act and how they emerge to create  
470 phenotypes, rational and predictable crop engineering may be achieved.

471

## 472 ACKNOWLEDGEMENTS

473 I thank Matthew Jackson and Iain Johnston for help creating images for the figures. G.W.B. was  
474 supported by BBSRC grants BB/J017604/1, BB/L010232/1, and BB/N009754/1, and  
475 Leverhulme Trust Grant RPG-2016-049.

476

## 477 TABLES

Method	Marker Visualization	Number of channels that can be visualized	Vital Marker Visualization	Subcellular resolution	Reference
mPA-PI	GUS	1	No	No	(Truernit et al., 2008)
ClearSee	Fluorescent	3-4	Yes	Yes	(Kurihara et al., 2015)
PEA-CLARITY	Fluorescent	24+	Yes	Yes	(Palmer et al., 2015)

478

479 **Table 1.** Summary of whole mount 3D imaging techniques for generating organ-wide cellular  
480 resolution images.

481

## 482 FIGURE and TABLE LEGENDS

483 **Table 1.** Summary of whole mount 3D imaging techniques for generating organ-wide cellular  
484 resolution images.

485 **Figure 1.** Workflow used to generate and analyse plant cellular interaction networks.

486 **Figure 2.** Schematic illustrating topological analyses of cellular interaction networks. (A)

487 Extraction of a connectivity network from a hypothetical network. (B) Degree is the number of

488 neighbours a cell has. (C) Betweenness centrality (BC) uses prior knowledge of the network to

489 find which nodes lie upon shortest paths between all other pairs of nodes. (D) Random Walk

490 Centrality (RWC) uses multiple random walkers to identify which cells lie upon shortest paths

491 between pairs of nodes. This does not use prior knowledge of the network to identify cells lying

492 upon shortest paths. (E) Navigation Centrality (NC) identifies near optimal shortest paths by

493 using local knowledge of a network while following a gradient to a destination node.

494 **Figure 3.** Illustrations highlighting differences between structural and functional networks. (A)

495 Structural network of a hypothetical tissue. (B) Functional annotation of cells (nodes) in the

496 network from (A) with the abundance of a cellular factor. The greyscale is proportional to the

497 abundance of this hypothetical component, indicated by the scale bar to the right having

498 arbitrary units. (C) Functional annotation of cell interfaces (edges) using the size of cell  
499 interfaces as a weighting. The size of the line width is proportional to the value.

500 **Figure 4.** Topological analysis of cellular organization in the *Arabidopsis* hypocotyl. (A)  
501 Annotation of cell types. (B) False colouring of cell degree. (C) False colouring of cell BC. (D)  
502 Concentration of fluorescein in distinct epidermal cell types of the hypocotyl. False colouring  
503 shows the relative concentration of fluorescence in each atrichoblast (a) and trichoblast (t) cells.  
504 (E) Model illustrating the division of labour between cell types in the hypocotyl epidermis. Large  
505 red arrows indicate the entry of solutes through hair cells (t). Small red arrows indicate the  
506 movement of solutes into adjacent non-hair cells (a) and their longitudinal movement is depicted  
507 by orange arrows.

508 **Figure 5.** Topological analysis of cellular organization in the 16 cell *Arabidopsis* embryo. (A)  
509 Connectivity network of the wild type 16 cell embryo and (B) the *RPS5A::bdl* expressing  
510 embryo. Cells (nodes) on the outside of the embryo are coloured green and those within the  
511 embryo yellow. The hypophysis is red and suspensor is in cyan. (C) Frequency distribution of  
512 shared neighbours between the wild type and *RPS5A::bdl* expressing embryo. Error bars  
513 represent the standard deviation of biological triplicates.

514  
515 **Figure 6.** Topological analysis of the *Arabidopsis* SAM. (A) Confocal stack of the SAM and  
516 extraction of a cellular connectivity network of the central region. (B) Geometric and topological  
517 cycling of cells which do not divide, cells which will divide, and cells which have divided in the  
518 SAM. (C) Computational prediction of cell division planes based on a local geometric rule  
519 (Errera), a rule which minimizes the degree of daughter cells, and a rule which minimizes the  
520 RWC of daughter cells. (D) Degree deviation from the observed cell division plane for each rule  
521 tested in (C). (E) Confocal image of the surface of a wild type SAM and (F) *ktn1* SAM. (G)  
522 Frequency distribution of cell anisotropy in the cells of the wild type and *ktn1* SAM. (H) Same as  
523 (G) for the RWC of cells. (I) Model describing emergence of global order in the SAM from the  
524 sensing of intercellular interactions by the cytoskeleton to minimization of RWC across the  
525 system.

526 of intercellular interactions by the cytoskeleton to minimization of RWC across the system.

527

## 528 REFERENCES

529 Assenov, Y., Ramírez, F., Schelhorn, S.-E., Lengauer, T., and Albrecht, M. (2007). Computing  
530 topological parameters of biological networks. *Bioinformatics* 24, 282-284.

- 531 Atwell, S., Huang, Y.S., Vilhjálmsson, B.J., Willems, G., Horton, M., Li, Y., Meng, D., Platt, A.,  
532 Tarone, A.M., and Hu, T.T. (2010). Genome-wide association study of 107 phenotypes in  
533 *Arabidopsis thaliana* inbred lines. *Nature* **465**, 627.
- 534 Avena-Koenigsberger, A., Goñi, J., Solé, R., and Sporns, O. (2015). Network morphospace. *J R*  
535 *Soc Interface* **12**, 20140881.
- 536 Baluška, F., and Levin, M. (2016). On having no head: cognition throughout biological systems.  
537 *Frontiers in psychology* **7**, 902.
- 538 Barabási, A.-L. (2016). *Network science* (Cambridge University Press).
- 539 Barthélemy, M. (2011). Spatial networks. *Physics Reports* **499**, 1-101.
- 540 Bassel, G.W. (2018). Information Processing and Distributed Computation in Plant Organs.  
541 *Trends in plant science*.
- 542 Bassel, G.W., and Smith, R.S. (2016). Quantifying morphogenesis in plants in 4D. *Current*  
543 *opinion in plant biology* **29**, 87-94.
- 544 Besson, S., and Dumais, J. (2011). Universal rule for the symmetric division of plant cells.  
545 *Proceedings of the National Academy of Sciences* **108**, 6294-6299.
- 546 Birnbaum, K.D. (2018). Power in Numbers: Single-Cell RNA-Seq Strategies to Dissect Complex  
547 Tissues. *Annu Rev Genet* **52**, 203-221.
- 548 Blilou, I., Xu, J., Wildwater, M., Willemsen, V., Paponov, I., Friml, J., Heidstra, R., Aida, M.,  
549 Palme, K., and Scheres, B. (2005). The PIN auxin efflux facilitator network controls growth and  
550 patterning in *Arabidopsis* roots. *Nature* **433**, 39-44.
- 551 Bonner, J.T. (1988). *The evolution of complexity by means of natural selection* (Princeton  
552 University Press).
- 553 Brunkard, J.O., and Zambryski, P.C. (2017). Plasmodesmata enable multicellularity: new  
554 insights into their evolution, biogenesis, and functions in development and immunity. *Current*  
555 *opinion in plant biology* **35**, 76-83.
- 556 Bullmore, E., and Sporns, O. (2009). Complex brain networks: graph theoretical analysis of  
557 structural and functional systems. *Nature Reviews Neuroscience* **10**, 186-198.
- 558 Carlsbecker, A., Lee, J.-Y., Roberts, C.J., Dettmer, J., Lehesranta, S., Zhou, J., Lindgren, O.,  
559 Moreno-Risueno, M.A., Vatén, A., and Thitamadee, S. (2010). Cell signalling by microRNA165/6  
560 directs gene dose-dependent root cell fate. *Nature* **465**, 316.
- 561 Carter, R., Sánchez-Corrales, Y.E., Hartley, M., Grieneisen, V.A., and Marée, A.F. (2017).  
562 Pavement cells and the topology puzzle. *Development* **144**, 4386-4397.
- 563 Chalfie, M., Sulston, J.E., White, J.G., Southgate, E., Thomson, J.N., and Brenner, S. (1985).  
564 The neural circuit for touch sensitivity in *Caenorhabditis elegans*. *Journal of Neuroscience* **5**,  
565 956-964.
- 566 Coen, E., Rolland-Lagan, A.G., Matthews, M., Bangham, J.A., and Prusinkiewicz, P. (2004).  
567 The genetics of geometry. *P Natl Acad Sci USA* **101**, 4728-4735.
- 568 Cuno, A., Esperanca, C., Oliveira, A., and Cavalcanti, P.R. (2004). Fast polygonization of  
569 variational implicit surfaces. *Xvii Brazilian Symposium on Computer Graphics and Image*  
570 *Processing, Proceedings*, 258-265.
- 571 de Reuille, P.B., Routier-Kierzkowska, A.-L., Kierzkowski, D., Bassel, G.W., Schüpbach, T.,  
572 Tauriello, G., Bajpai, N., Strauss, S., Weber, A., and Kiss, A. (2015). MorphoGraphX: a platform  
573 for quantifying morphogenesis in 4D. *Elife* **4**, e05864.
- 574 De Smet, I., and Beeckman, T. (2011). Asymmetric cell division in land plants and algae: the  
575 driving force for differentiation. *Nat Rev Mol Cell Bio* **12**, 177.
- 576 DiLaurenzio, L., WysockaDiller, J., Malamy, J.E., Pysh, L., Helariutta, Y., Freshour, G., Hahn,  
577 M.G., Feldmann, K.A., and Benfey, P.N. (1996). The SCARECROW gene regulates an  
578 asymmetric cell division that is essential for generating the radial organization of the *Arabidopsis*  
579 root. *Cell* **86**, 423-433.
- 580 Dissmeyer, N., Weimer, A.K., Pusch, S., De Schutter, K., Kamei, C.L.A., Nowack, M.K., Novak,  
581 B., Duan, G.-L., Zhu, Y.-G., and De Veylder, L. (2009). Control of cell proliferation, organ

582 growth, and DNA damage response operate independently of dephosphorylation of the  
583 Arabidopsis Cdk1 homolog CDKA; 1. *The Plant Cell* 21, 3641-3654.

584 Dolan, L. (2005). Positional information and mobile transcriptional regulators determine cell  
585 pattern in the Arabidopsis root epidermis. *Journal of experimental botany* 57, 51-54.

586 Dong, J., MacAlister, C.A., and Bergmann, D.C. (2009). BASL controls asymmetric cell division  
587 in Arabidopsis. *Cell* 137, 1320-1330.

588 Doursat, R., Sayama, H., and Michel, O. (2012). Morphogenetic engineering: toward  
589 programmable complex systems (Springer).

590 Duckett, C., Grierson, C., Linstead, P., Schneider, K., Lawson, E., Dean, C., Poethig, S., and  
591 Roberts, K. (1994). Clonal relationships and cell patterning in the root epidermis of Arabidopsis.  
592 *Development* 120, 2465-2474.

593 Duran-Nebreda, S., and Bassel, G.W. (2017a). Bridging Scales in Plant Biology Using Network  
594 Science. *Trends in plant science*.

595 Duran-Nebreda, S., and Bassel, G.W. (2017b). Fluorescein Transport Assay to Assess Bulk  
596 Flow of Molecules Through the Hypocotyl in Arabidopsis thaliana. *eLIFE*.

597 Errera, L. (1888). Über zellformen und seifenblasen. *Bot Centralbl* 34, 395-398.

598 Fang, S.Q., Clark, R.T., Zheng, Y., Iyer-Pascuzzi, A.S., Weitz, J.S., Kochian, L.V.,  
599 Edelsbrunner, H., Liao, H., and Benfey, P.N. (2013). Genotypic recognition and spatial  
600 responses by rice roots. *P Natl Acad Sci USA* 110, 2670-2675.

601 Fernandez, R., Das, P., Mirabet, V., Moscardi, E., Traas, J., Verdeil, J.L., Malandain, G., and  
602 Godin, C. (2010). Imaging plant growth in 4D: robust tissue reconstruction and lineaging at cell  
603 resolution. *Nat Methods* 7, 547-553.

604 Fitzgibbon, J., Beck, M., Zhou, J., Faulkner, C., Robatzek, S., and Oparka, K. (2013). A  
605 developmental framework for complex plasmodesmata formation revealed by large-scale  
606 imaging of the Arabidopsis leaf epidermis. *The Plant Cell* 25, 57-70.

607 Freeman, L.C. (1977). A set of measures of centrality based on betweenness. *Sociometry*, 35-  
608 41.

609 Gaillochet, C., Daum, G., and Lohmann, J.U. (2015). O cell, where art thou? The mechanisms  
610 of shoot meristem patterning. *Current Opinion in Plant Biology* 23, 91-97.

611 Gendreau, E., Traas, J., Desnos, T., Grandjean, O., Caboche, M., and Hofte, H. (1997). Cellular  
612 basis of hypocotyl growth in Arabidopsis thaliana. *Plant physiology* 114, 295-305.

613 Gerlitz, N., Gerum, R., Sauer, N., and Stadler, R. (2018). Photoinducible DRONPA-s: a new tool  
614 for investigating cell-cell connectivity. *The Plant Journal* 94, 751-766.

615 Gibson, M.C., Patel, A.B., Nagpal, R., and Perrimon, N. (2006). The emergence of geometric  
616 order in proliferating metazoan epithelia. *Nature* 442, 1038-1041.

617 Gibson, W.T., and Gibson, M.C. (2009). Cell topology, geometry, and morphogenesis in  
618 proliferating epithelia. *Current topics in developmental biology* 89, 87-114.

619 Gibson, W.T., Veldhuis, J.H., Rubinstein, B., Cartwright, H.N., Perrimon, N., Brodland, G.W.,  
620 Nagpal, R., and Gibson, M.C. (2011). Control of the mitotic cleavage plane by local epithelial  
621 topology. *Cell* 144, 427-438.

622 Halpern, K.B., Shenhav, R., Matcovitch-Natan, O., Tóth, B., Lemze, D., Golan, M., Massasa,  
623 E.E., Baydatch, S., Landen, S., and Moor, A.E. (2017). Single-cell spatial reconstruction reveals  
624 global division of labour in the mammalian liver. *Nature* 542, 352.

625 Hamann, T., Benkova, E., Bäurle, I., Kientz, M., and Jürgens, G. (2002). The Arabidopsis  
626 BODENLOS gene encodes an auxin response protein inhibiting MONOPTEROS-mediated  
627 embryo patterning. *Genes & development* 16, 1610-1615.

628 Hamant, O., Heisler, M.G., Jonsson, H., Krupinski, P., Uyttewaal, M., Bokov, P., Corson, F.,  
629 Sahlin, P., Boudaoud, A., Meyerowitz, E.M., *et al.* (2008). Developmental Patterning by  
630 Mechanical Signals in Arabidopsis. *Science* 322, 1650-1655.

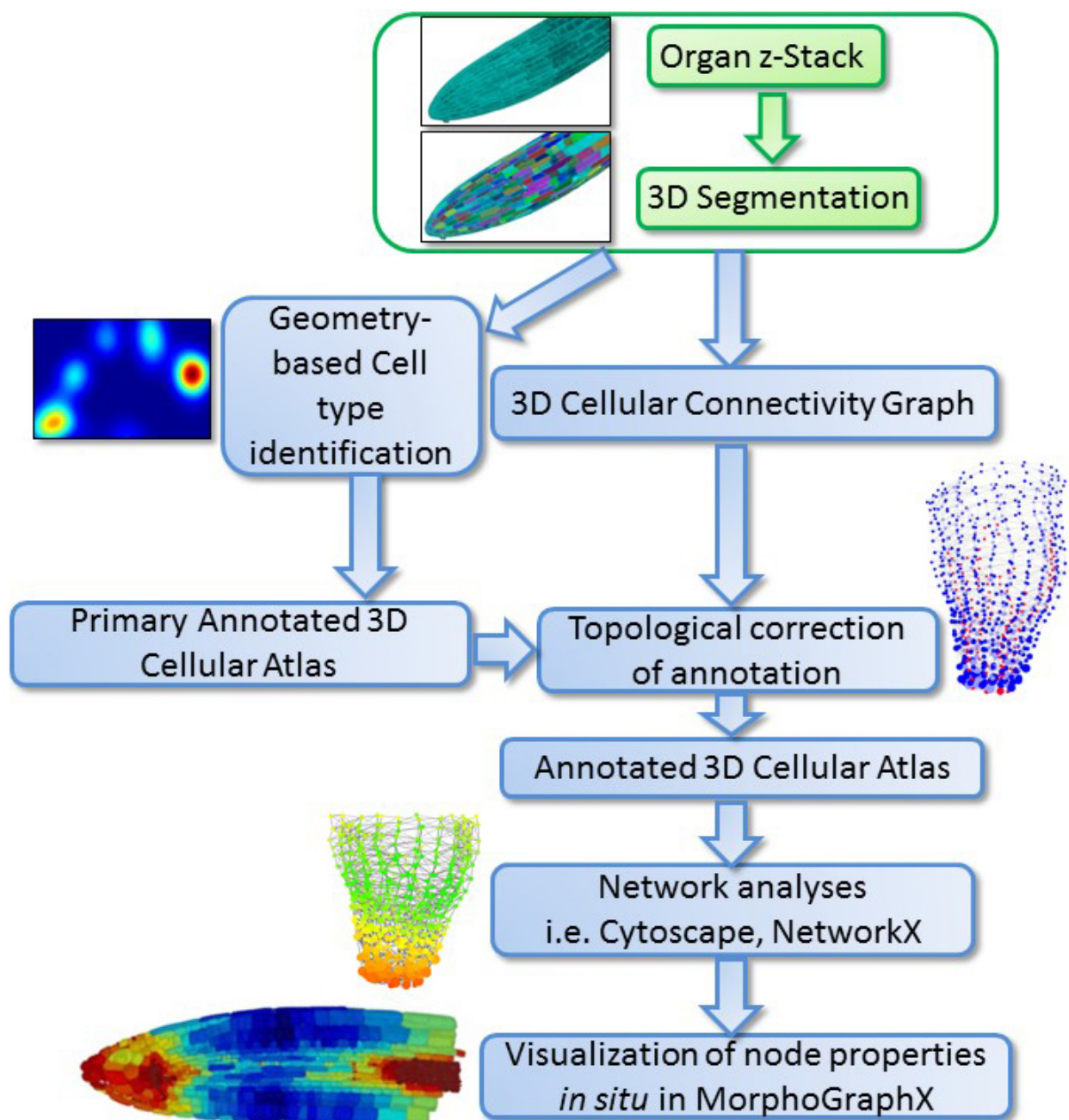


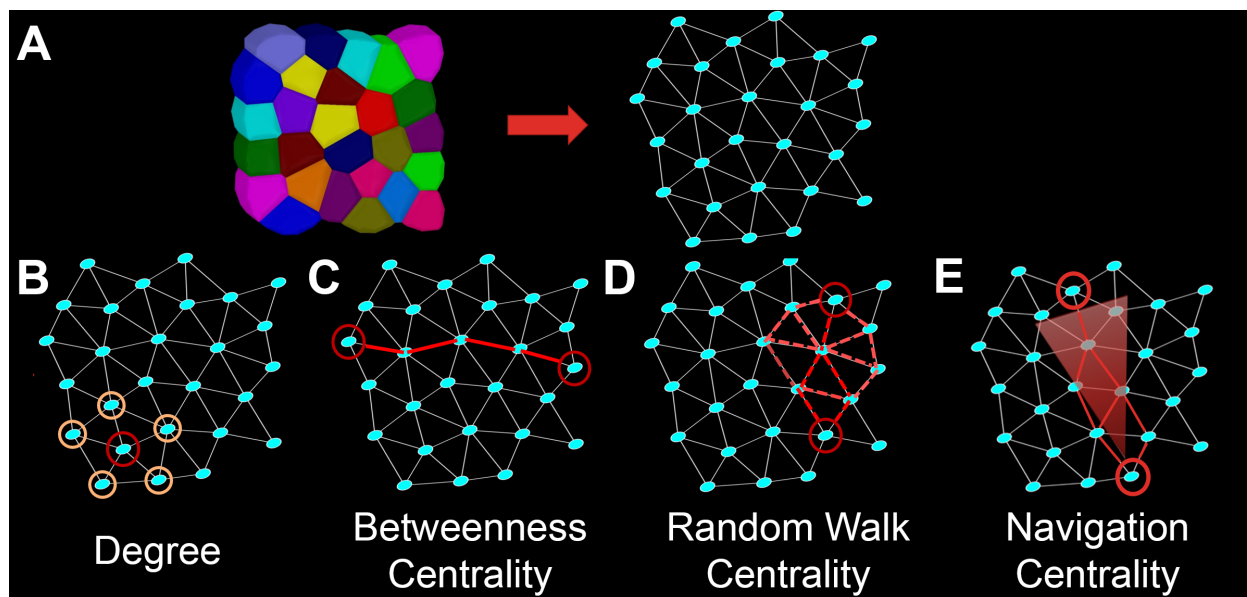
- 631 Hardtke, C.S., and Berleth, T. (1998). The Arabidopsis gene MONOPTEROS encodes a  
632 transcription factor mediating embryo axis formation and vascular development. *The EMBO*  
633 *journal* 17, 1405-1411.
- 634 Holme, P., and Saramäki, J. (2012). Temporal networks. *Physics reports* 519, 97-125.
- 635 Jackson, M.D., Duran-Nebreda, S., and Bassel, G.W. (2017a). Network-based approaches to  
636 quantify multicellular development. *J R Soc Interface* 14, 20170484.
- 637 Jackson, M.D., Duran-Nebreda, S., Kierzkowski, D., Strauss, S., Xu, H., Landrein, B., Hamant,  
638 O., Smith, R.S., Johnston, I.G., and Bassel, G.W. (2019). Global Topological Order Emerges  
639 through Local Mechanical Control of Cell Divisions in the Arabidopsis Shoot Apical Meristem.  
640 *Cell Systems*.
- 641 Jackson, M.D., Xu, H., Duran-Nebreda, S., Stamm, P., and Bassel, G.W. (2017b). Topological  
642 analysis of multicellular complexity in the plant hypocotyl. *eLife* 6.
- 643 Jones, A.R., Forero-Vargas, M., Withers, S.P., Smith, R.S., Traas, J., Dewitte, W., and Murray,  
644 J.A. (2017). Cell-size dependent progression of the cell cycle creates homeostasis and flexibility  
645 of plant cell size. *Nat Commun* 8.
- 646 Kierzkowski, D., Nakayama, N., Routier-Kierzkowska, A.L., Weber, A., Bayer, E., Schorderet,  
647 M., Reinhardt, D., Kuhlemeier, C., and Smith, R.S. (2012). Elastic Domains Regulate Growth  
648 and Organogenesis in the Plant Shoot Apical Meristem. *Science* 335, 1096-1099.
- 649 Knight, M.R., Campbell, A.K., Smith, S.M., and Trewavas, A.J. (1991). Transgenic plant  
650 aequorin reports the effects of touch and cold-shock and elicitors on cytoplasmic calcium.  
651 *Nature* 352, 524.
- 652 Kubo, M., Nishiyama, T., Tamada, Y., Sano, R., Ishikawa, M., Murata, T., Imai, A., Lang, D.,  
653 Demura, T., and Reski, R. (2018). Single-cell transcriptome analysis of *Physcomitrella* leaf cells  
654 during reprogramming using microcapillary manipulation. *bioRxiv*, 463448.
- 655 Kurihara, D., Mizuta, Y., Sato, Y., and Higashiyama, T. (2015). ClearSee: a rapid optical  
656 clearing reagent for whole-plant fluorescence imaging. *Development, dev.* 127613.
- 657 Latora, V., and Marchiori, M. (2001). Efficient behavior of small-world networks. *Physical review*  
658 *letters* 87, 198701.
- 659 Lucas, W.J., Bouché-Pillon, S., Jackson, D.P., and Nguyen, L. (1995). Selective trafficking of  
660 KNOTTED1 homeodomain protein and its mRNA through plasmodesmata. *Science* 270, 1980.
- 661 Lucas, W.J., and Lee, J.-Y. (2004). Plasmodesmata as a supracellular control network in plants.  
662 *Nat Rev Mol Cell Bio* 5, 712-726.
- 663 Meyerowitz, E.M. (1997). Genetic control of cell division patterns in developing plants. *Cell* 88,  
664 299-308.
- 665 Montenegro-Johnson, T.D., Stamm, P., Strauss, S., Topham, A.T., Tsagris, M., Wood, A.T.,  
666 Smith, R.S., and Bassel, G.W. (2015). Digital single-cell analysis of plant organ development  
667 using 3DCellAtlas. *The Plant Cell* 27, 1018-1033.
- 668 Muscoloni, A., and Cannistraci, C.V. (2019). Navigability evaluation of complex networks by  
669 greedy routing efficiency. *Proceedings of the National Academy of Sciences* 116, 1468-1469.
- 670 Muscoloni, A., Thomas, J.M., Ciucci, S., Bianconi, G., and Cannistraci, C.V. (2017). Machine  
671 learning meets complex networks via coalescent embedding in the hyperbolic space. *Nat*  
672 *Commun* 8, 1615.
- 673 Nakajima, K., Sena, G., Nawy, T., and Benfey, P.N. (2001). Intercellular movement of the  
674 putative transcription factor SHR in root patterning. *Nature* 413, 307-311.
- 675 Newman, M. (2010). *Networks: an introduction* (Oxford university press).
- 676 Newman, M.E. (2005). A measure of betweenness centrality based on random walks. *Social*  
677 *networks* 27, 39-54.
- 678 Ogawa, M., Shinohara, H., Sakagami, Y., and Matsubayashi, Y. (2008). Arabidopsis CLV3  
679 peptide directly binds CLV1 ectodomain. *Science* 319, 294-294.

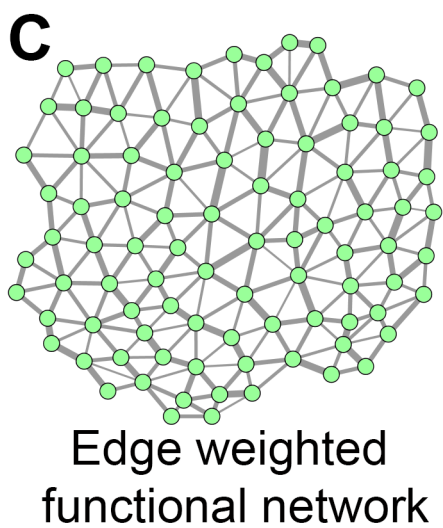
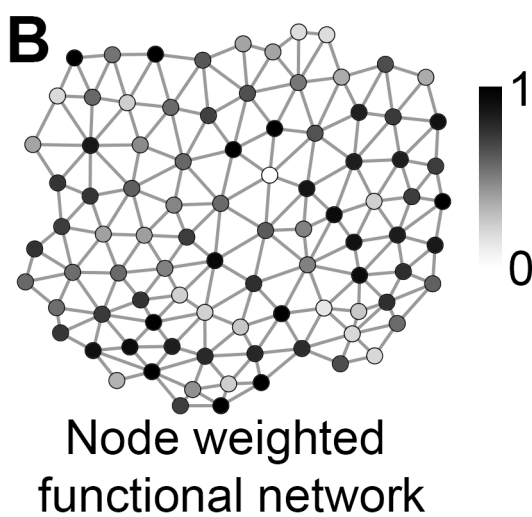
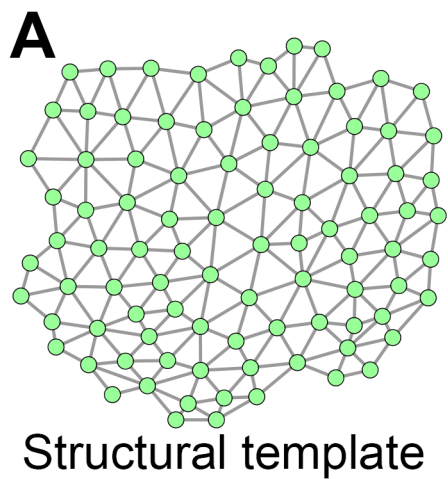
- 680 Ollé-Vila, A., Duran-Nebreda, S., Conde-Pueyo, N., Montañez, R., and Solé, R. (2016). A  
681 morphospace for synthetic organs and organoids: the possible and the actual. *Integr Biol-Uk* 8,  
682 485-503.
- 683 Palmer, W.M., Martin, A.P., Flynn, J.R., Reed, S.L., White, R.G., Furbank, R.T., and Grof, C.P.  
684 (2015). PEA-CLARITY: 3D molecular imaging of whole plant organs. *Scientific reports* 5.
- 685 Pincus, Z., and Theriot, J. (2007). Comparison of quantitative methods for cell-shape analysis.  
686 *Journal of microscopy* 227, 140-156.
- 687 Raissig, M.T., Matos, J.L., Gil, M.X.A., Kornfeld, A., Bettadapur, A., Abrash, E., Allison, H.R.,  
688 Badgley, G., Vogel, J.P., and Berry, J.A. (2017). Mobile MUTE specifies subsidiary cells to build  
689 physiologically improved grass stomata. *Science* 355, 1215-1218.
- 690 Ramon y Cajal, S. (1911). *Histologie du Systeme Nerveux de l'homme et des Vertebres*, Vol. 2.  
691 Maloine, Paris, 887-890.
- 692 Rinne, P.L., Kaikuranta, P.M., and van der Schoot, C. (2001). The shoot apical meristem  
693 restores its symplasmic organization during chilling-induced release from dormancy. *Plant J* 26,  
694 249-264.
- 695 Rinne, P.L., Welling, A., Vahala, J., Ripel, L., Ruonala, R., Kangasjarvi, J., and van der Schoot,  
696 C. (2011). Chilling of dormant buds hyperinduces FLOWERING LOCUS T and recruits GA-  
697 inducible 1,3-beta-glucanases to reopen signal conduits and release dormancy in *Populus*.  
698 *Plant Cell* 23, 130-146.
- 699 Roeder, A.H.K., Cunha, A., Burl, M.C., and Meyerowitz, E.M. (2012). A computational image  
700 analysis glossary for biologists. *Development* 139, 3071-3080.
- 701 Roeder, A.H.K., Tarr, P.T., Tobin, C., Zhang, X.L., Chickarmane, V., Cunha, A., and  
702 Meyerowitz, E.M. (2011). Computational morphodynamics of plants: integrating development  
703 over space and time. *Nat Rev Mol Cell Bio* 12, 265-+.
- 704 Ryan, K., Lu, Z., and Meinertzhagen, I.A. (2016). The CNS connectome of a tadpole larva of  
705 *Ciona intestinalis* (L.) highlights sidedness in the brain of a chordate sibling. *Elife* 5, e16962.
- 706 Sahlin, P., and Jönsson, H. (2010). A modeling study on how cell division affects properties of  
707 epithelial tissues under isotropic growth. *PloS one* 5, e11750.
- 708 Sánchez-Corrales, Y.E., Hartley, M., van Rooij, J., Marée, A.F., and Grieneisen, V.A. (2018).  
709 Morphometrics of complex cell shapes: lobe contribution elliptic Fourier analysis (LOCO-EFA).  
710 *Development, dev.* 156778.
- 711 Schlereth, A., Möller, B., Liu, W., Kientz, M., Flipse, J., Rademacher, E.H., Schmid, M., Jürgens,  
712 G., and Weijers, D. (2010). MONOPTEROS controls embryonic root initiation by regulating a  
713 mobile transcription factor. *Nature* 464, 913-916.
- 714 Seguin, C., van den Heuvel, M.P., and Zalesky, A. (2018). Navigation of brain networks.  
715 *Proceedings of the National Academy of Sciences*, 201801351.
- 716 Sliwinska, E., Bassel, G.W., and Bewley, J.D. (2009). Germination of *Arabidopsis thaliana*  
717 seeds is not completed as a result of elongation of the radicle but of the adjacent transition zone  
718 and lower hypocotyl. *J Exp Bot* 60, 3587-3594.
- 719 Smith, L.G. (2001). Cell division: Plant cell division: building walls in the right places. *Nat Rev*  
720 *Mol Cell Bio* 2, 33.
- 721 Solé, R., and Goodwin, B. (2000). *How complexity pervades biology*. New York: Basic.
- 722 Solé, R., Ollé-Vila, A., Vidiella, B., Duran-Nebreda, S., and Conde-Pueyo, N. (2018). The road  
723 to synthetic multicellularity. *Current Opinion in Systems Biology*.
- 724 Sporns, O., Tononi, G., and Kötter, R. (2005). The human connectome: a structural description  
725 of the human brain. *PLoS computational biology* 1, e42.
- 726 Swarup, R., Friml, J., Marchant, A., Ljung, K., Sandberg, G., Palme, K., and Bennett, M. (2001).  
727 Localization of the auxin permease AUX1 suggests two functionally distinct hormone transport  
728 pathways operate in the *Arabidopsis* root apex. *Genes & development* 15, 2648-2653.

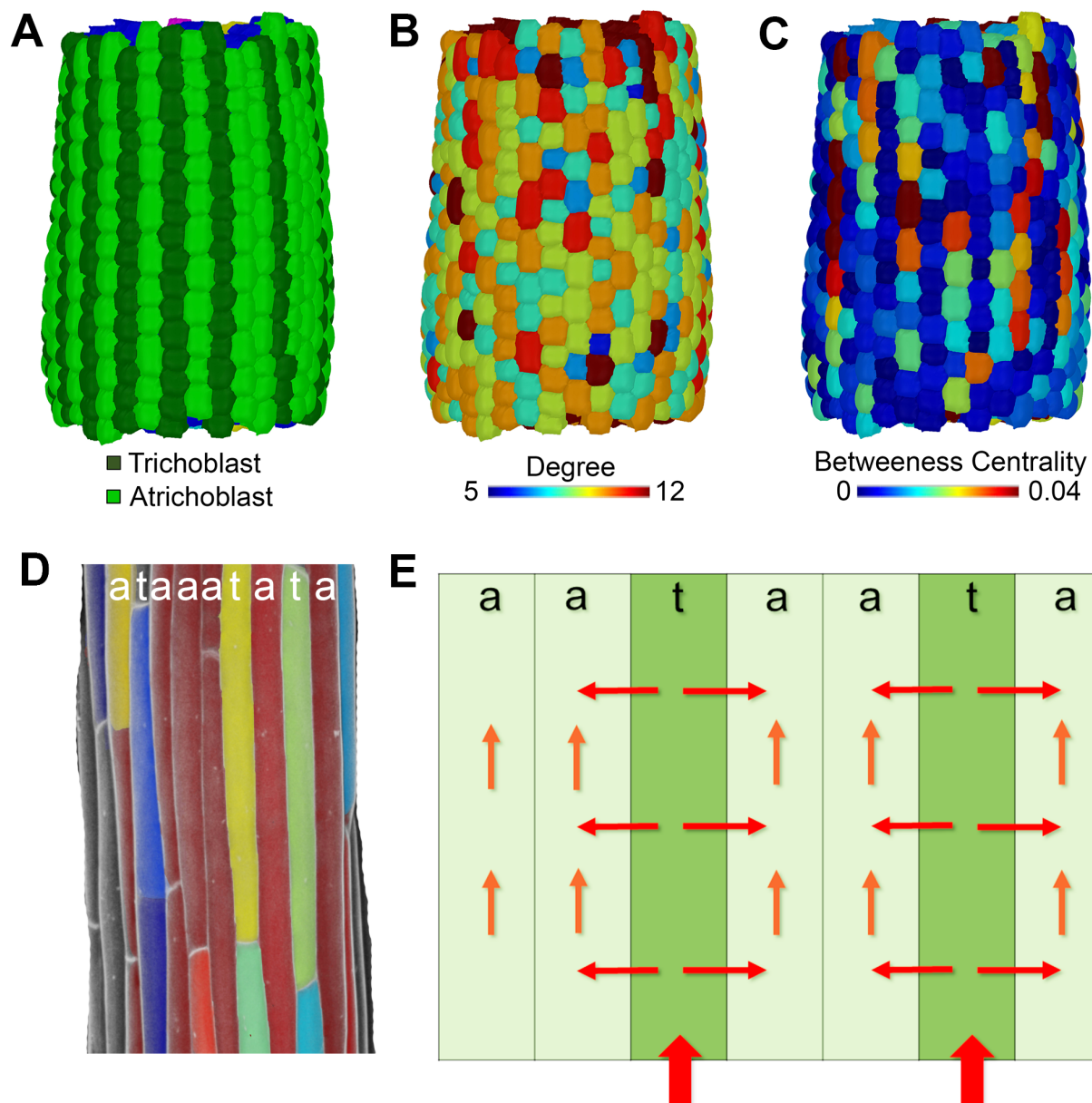
- 729 Tal, I., Zhang, Y., Jørgensen, M.E., Pisanty, O., Barbosa, I.C., Zourelidou, M., Regnault, T.,  
730 Crocoll, C., Olsen, C.E., and Weinstain, R. (2016). The Arabidopsis NPF3 protein is a GA  
731 transporter. *Nat Commun* 7.
- 732 Thompson, D.W. (1942). On growth and form. On growth and form.
- 733 Truernit, E., Bauby, H., Dubreucq, B., Grandjean, O., Runions, J., Barthelemy, J., and Palauqui,  
734 J.C. (2008). High-resolution whole-mount imaging of three-dimensional tissue organization and  
735 gene expression enables the study of Phloem development and structure in Arabidopsis. *Plant*  
736 *Cell* 20, 1494-1503.
- 737 Uyttewaal, M., Burian, A., Alim, K., Landrein, B.T., Borowska-Wykret, D., Dedieu, A., Peaucelle,  
738 A., Ludynia, M., Traas, J., Boudaoud, A., *et al.* (2012). Mechanical Stress Acts via Katanin to  
739 Amplify Differences in Growth Rate between Adjacent Cells in Arabidopsis. *Cell* 149, 439-451.
- 740 Von Mering, C., Krause, R., Snel, B., Cornell, M., Oliver, S.G., Fields, S., and Bork, P. (2002).  
741 Comparative assessment of large-scale data sets of protein–protein interactions. *Nature* 417,  
742 399.
- 743 White, J.G., Southgate, E., Thomson, J.N., and Brenner, S. (1986). The structure of the nervous  
744 system of the nematode *Caenorhabditis elegans*. *Philos Trans R Soc Lond B Biol Sci* 314, 1-  
745 340.
- 746 Willis, L., Refahi, Y., Wightman, R., Landrein, B., Teles, J., Huang, K.C., Meyerowitz, E.M., and  
747 Jönsson, H. (2016). Cell size and growth regulation in the Arabidopsis thaliana apical stem cell  
748 niche. *Proceedings of the National Academy of Sciences* 113, E8238-E8246.
- 749 Yan, G., Vértes, P.E., Towilson, E.K., Chew, Y.L., Walker, D.S., Schafer, W.R., and Barabási,  
750 A.-L. (2017). Network control principles predict neuron function in the *Caenorhabditis elegans*  
751 connectome. *Nature* 550, 519.
- 752 Yoshida, S., de Reuille, P.B., Lane, B., Bassel, G.W., Prusinkiewicz, P., Smith, R.S., and  
753 Weijers, D. (2014). Genetic Control of Plant Development by Overriding a Geometric Division  
754 Rule. *Dev Cell* 29, 75-87.
- 755











ACCEPTED

